DAΦNE TECHNICAL NOTE

INFN - LNF, Accelerator Division

Frascati, March 11, 2008

Note: **L-39**

BEAM TRAJECTORY INSIDE THE MODIFIED DIPOLES FOR THE DAΦNE UPGRADE

M. Preger, S. Tomassini

1. Introduction

The reasons for the modification of the DAΦNE lattice for the upgrade realized in fall 2007 are explained in [1], where the changes in the interaction region and adjacent dipoles geometry are also described. However, the layout presented in [1] is schematic, while the real position of the dipoles with respect to the vacuum chamber has undergone non negligible modifications in order to cope with the shape of the vacuum chamber itself and optimize matching with the interaction region straight sections. This report presents the results of the beam trajectory calculation, performed on the measured field maps and compared with the position of the vacuum chamber.

2. Present layout

Figure 1 shows the layout of the two dipoles adjacent to the interaction region. The position of the large vacuum chamber of the arcs has not been changed, while the dipoles have been moved with respect to the previous position. The points indicated with C0 in Figure 1 represent the positions of the old center of curvature of the two dipoles. The circular sector representing the old dipole positions is shown in red. This sector is also the center of the dipole vacuum chamber in the present position, since the large vacuum chamber in the arcs of DAΦNE has not been moved. The black sector shows instead the new position of the dipoles, and their center of curvature are indicated with P0. C1 and P1 are the points where the straight section of the arc crosses the dipole arc in the old and in the new configuration respectively, while C2 and P2 are the corresponding positions where the dipole arc crosses the straight section in the interaction region. C3 is the center of the flange at the end of the large arc vacuum chamber, which is now connected to the interaction vacuum chamber by means of a short asymmetric matching pipe. The latter ends with a flange connected to the new bellows at the end of the interaction region vacuum chamber. The center of this flange is indicated with C4. Finally C5 is a generic point on the axis of the interaction region vacuum chamber, necessary to establish the direction of the beam as explained in the following.

The coordinates of the points in the figure are referred to the machine reference system (MRS) with the origin at the center of the collider, the horizontal axis from the origin to the interaction point and the vertical axis from the origin to the center of the injection straight section. The available field maps of the dipoles are taken instead on the magnetic measurement reference system (DRS) with the origin in the dipole center of curvature and the vertical axis on the nominal entrance radius of the dipole. In order to track a test particle through the field map, it is therefore necessary to perform two transformations of coordinates, the first from the MRS to the DRS of the long sector dipole, the second from the MRS to the DRS of the short one. Table 1 and 2 give the coordinates of the above described points in the three reference systems.

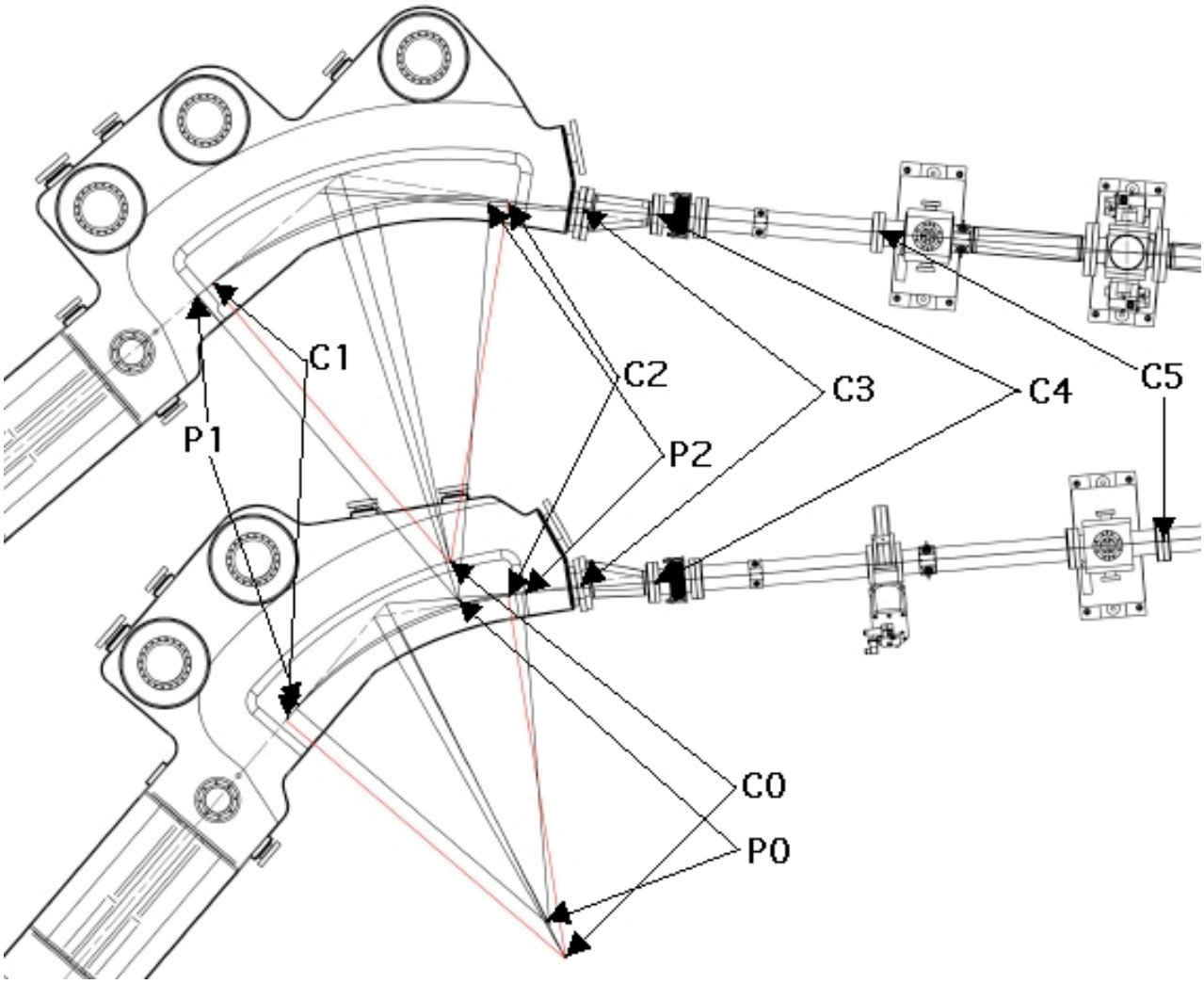

Figure 1 – Layout of the modified dipoles.

The transformation of coordinates from MRS to DRS for the long dipole is:

$$x_{DRS} = 0.675101\left(x_{MRS} - 11.01483\right) - 0.737726\left(y_{MRS} - 10.38253\right)$$
$$y_{DRS} = 0.737726\left(x_{MRS} - 11.01483\right) + 0.675101\left(y_{MRS} - 10.38253\right)$$

while the corresponding one for the short dipole is:

$$x_{DRS} = 0.735538\left(x_{MRS} - 9.53426\right) - 0.677483\left(y_{MRS} - 9.93007\right)$$
$$y_{DRS} = 0.677483\left(x_{MRS} - 9.53426\right) + 0.735538\left(y_{MRS} - 9.93007\right)$$

These transformations consist in a translation from the center of the machine to the curvature center of the dipoles in the new position and a rotation by 47.538° for the long dipole and 42.647° for the short one.

Table 1 – Coordinates of the reference points for the short dipole.

	MRS hor. (m)	**MRS vert. (m)**	**DRS hor.(m)**	**DRS vert. (m)**
C0	9.52059	9.92922	-0.00948	-0.00989
P0	9.53426	9.93007	0	0
C1	10.43018	10.99422	-0.06196	1.38969
P1	10.48312	10.96024	0	1.40056
C2	10.90391	10.14832	0.85957	1.08845
P2	10.92481	10.09718	0.90959	1.06499
C3	10.94920	9.86304	1.08615	0.90929
C4	10.95667	9.59247	1.27495	0.71534
C5	11.11286	7.65526	2.70227	-0.60373

Table 2 – Coordinates of the reference points for the long dipole.

	MRS hor. (m)	**MRS vert. (m)**	**DRS hor.(m)**	**DRS vert. (m)**
C0	11.02933	10.36742	0.02094	0.00050
P0	11.01483	10.38253	0	0
C1	12.09433	11.27701	0.06889	1.40024
P1	12.04806	11.32805	0	1.40056
C2	12.41267	10.14832	1.11647	0.87311
P2	12.40483	10.21092	1.06499	0.90959
C3	12.36744	9.86171	1.29737	0.64625
C4	12.36185	9.61410	1.47627	0.47496
C5	12.29123	8.73880	2.07432	-0.16805

3. Results

There are some significant differences between the real conditions for the tracking given by the positions shown in Figure 1 and Tables 1 and 2 and the schematic layout assumed in [1]. The beam enters the real dipole at an angle of 1.96° and its exit angle is 2.42° in the case of the long dipole; its offset at the entrance is 2.04 mm with respect to the ideal vertex of the sector towards the outside of the ring. In the case treated in [1] both angles were 2.19°. In the case of the short dipole the corresponding quantities are 2.15°, 2.24° and -8.54 mm. The short dipole is therefore placed more symmetrically with respect to the old configuration.

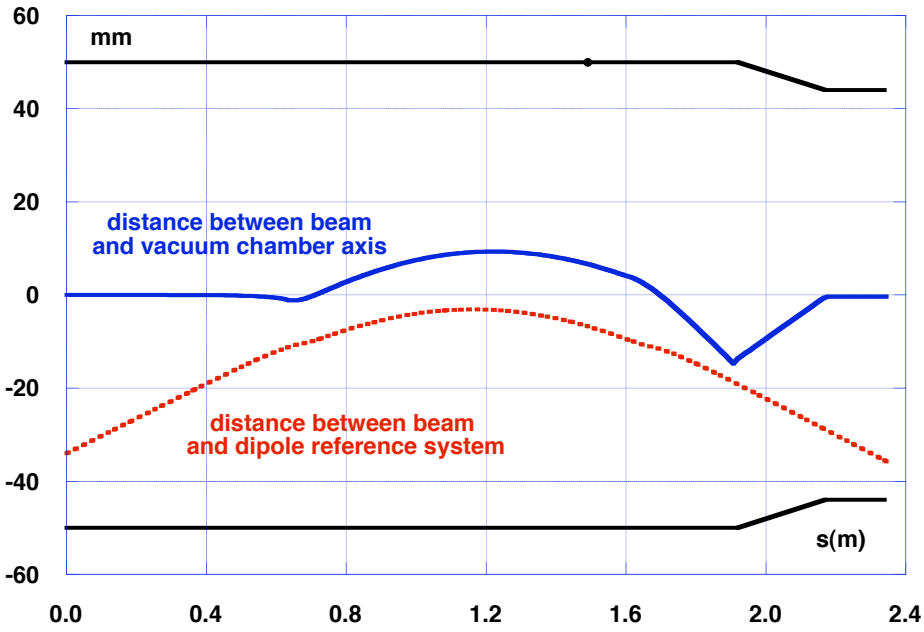

Figure 2 – Beam trajectory in the short dipole.

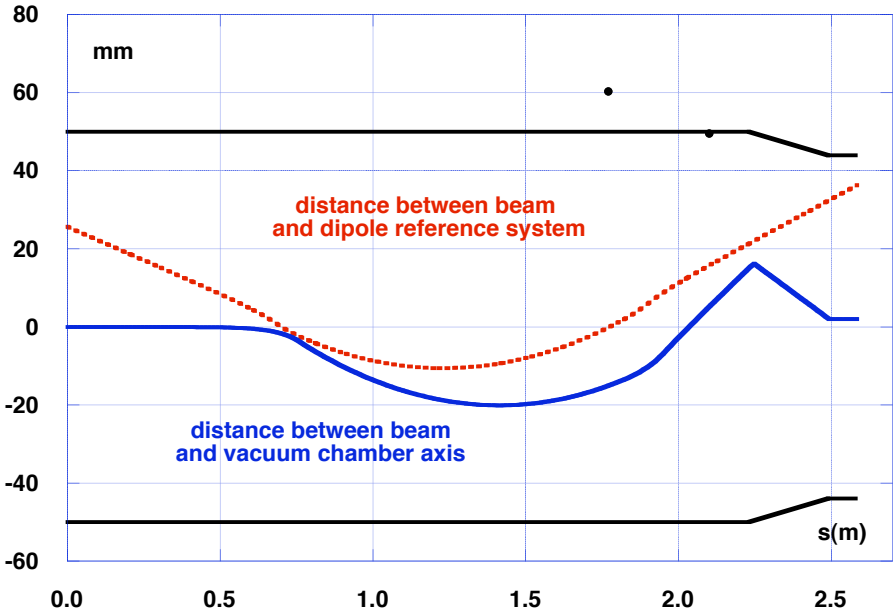

Figure 3 – Beam trajectory in the long dipole.

Figures 2 and 3 show the results of the particle tracking for the short and long dipole respectively. The dotted red line shows the distance of the particle trajectory from the nominal trajectory in the old configuration, namely a circular arc with the nominal radius (1.40056 m) and bending angles (49.5° for the long dipole and 40.5° for the short one) and two straight sections tangent to the arc itself. The full blue line shows instead the distance between the particle trajectory and the center of the vacuum chamber. The discontinuity in its derivative is due to a corresponding discontinuity in the center of the vacuum chamber at the points where the long chamber in the arcs matches the new chamber in the interaction regions.

The black lines in the figures show the position of the beam stay clear in the chamber. The beam is offset by -13.7 mm in the short dipole and +16.2 mm in the long one in the flange of the long vacuum chamber in the arc. In the center of the dipole the maximum offset from the center of the chamber is +9.3 mm for the short dipole, -20.1 mm for the long one. The offset of the beam at the entrance of the interaction region chamber is -0.3 mm for the short dipole, +2.0 mm for the long one. The small black dots near the outer part of the stay clear line represent the positions of the synchrotron radiation absorbers nearest to the beam.

Figure 4 shows the same tracking performed on a map of the long dipole taken after removing the iron end caps. The maximum offset inside the dipole drops to -16.6 mm, while the offset at the flange at the end of the long vacuum chamber of the arcs does not change much (16.6 mm instead of 16.2).

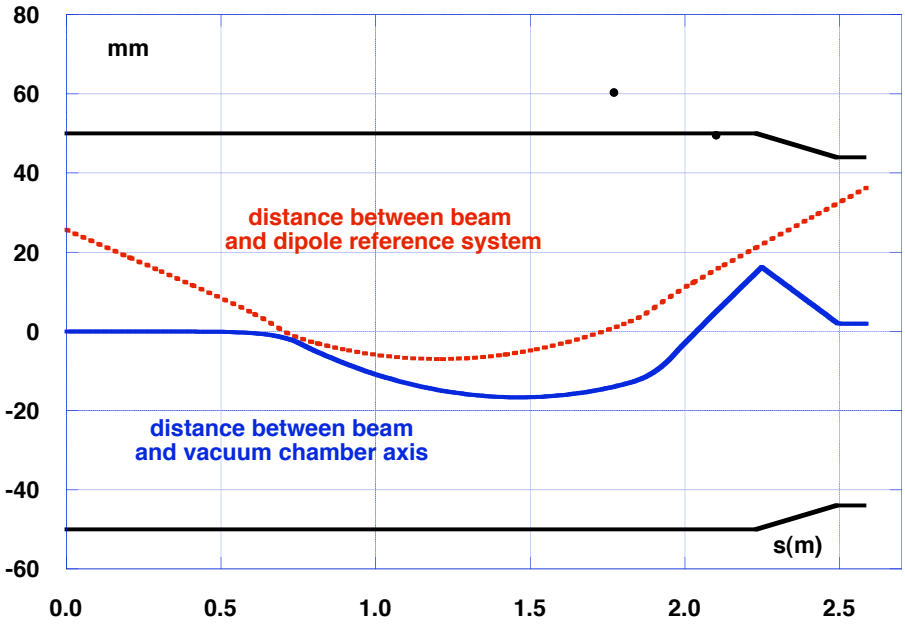

Figure 4 – Beam trajectory in the long dipole without end caps.

4. Effects on the optical model and excitation currents

Due to the significant differences with respect to the geometry assumed in [1], there are some differences in the parameters of the optical model. In fact, for the long dipole, the rotation of the dipole with respect to the old configuration is such that the trajectory is no more symmetric with respect to the center of the magnet, and therefore the matrix element a_{11} is different from a_{22}. The difference is 5.9×10^{-3}, ≈4 times larger than in [1]. To obtain the same average difference between the "tracked" and "optical" matrices, it is now necessary to have different entrance and exit angles in dipole model. We find a best entrance angle of -0.012 rad (-0.69°) and a best exit angle of -0.022 rad (-1.26°). The entrance is on the side of the arc straight section, the exit on the side of the interaction region.

In the case of the short dipole the difference is smaller, since its new position is more symmetric. We find a best entrance angle of 0.048 rad (2.75°) and a best exit angle of 0.044 rad (2.52°). The accuracy of the determinant is better than 10^{-3} for both dipoles.

The calculation of the excitation current in the dipoles has also been repeated under the new geometrical conditions. The result is shown in the following table.

Table 3 – Excitation current in the dipoles.

	Required field integral (Tm)	**Interpolated current (A)**
PES	1.20229	264.6
SLL	1.33921	234.4
SLS	1.33254	313.9

REFERENCES

[1] M. Preger: "Optical Model for the DAΦNE Upgrade", DAΦNE Technical Note L-38, 6/11/07.